Proceedings of the ASME 2020 Dynamic Systems and Control Conference
DSCC 2020
October 4-7, 2020, Pittsburgh, Pennsylvania, USA

DSCC2020-20867

EXPERIMENTAL AND ANALYTICAL DECENTRALIZED ADAPTIVE CONTROL OF A 7-DOF ROBOT MANIPULATOR

Alexander Bertino
Research Assistant
Dynamic Systems and Control Lab.
Dept. of Mechanical Eng.
San Diego State University
San Diego, California 92182
Email: abertino6245@sdsu.edu

Peiman Naseradinmousavi
Associate Professor
Dynamic Systems and Control Lab.
Dept. of Mechanical Eng.
San Diego State University
San Diego, California 92182
Email: pnaseradinmousavi@sdsu.edu

Atul Kelkar
D. W. Reynolds Distinguished Professor
Department Chair of Mechanical Eng.
Clemson University
Clemson, South Carolina 29632
Email: atul@clemson.edu

ABSTRACT

In this paper, we study the analytical and experimental control of a 7-DOF robot manipulator. A model-free decentralized adaptive control strategy is presented for the tracking control of the manipulator. The problem formulation and experimental results demonstrate the computational efficiency and simplicity of the proposed method. The results presented here are one of the first known experiments on a redundant 7-DOF robot. The efficacy of the adaptive decentralized controller is demonstrated experimentally by using the Baxter robot to track a desired trajectory. Simulation and experimental results clearly demonstrate the versatility, tracking performance, and computational efficiency of this method.

1 Introduction

As the global trend is towards increased automation, robot manipulators have seen widespread use in many industrial applications. While the research in adaptive and nonlinear control has seen significant advances, most robot manipulators utilized in industry are driven by simple decentralized PID controllers due to their simplicity in their design and implementation [1, 2]. While these controllers are effective at driving robot manipulators to specific set points, they have difficulty in tracking an arbitrary desired trajectory. Furthermore, due to the strong interconnected nonlinearities inherently present in the dynamic model of such systems, a given set of PID gains will only work well for a specific joint configuration and end-effector mass. While many pick-and-place type operations in industry not needing navigation through obstacles can be performed effectively using PID type controllers, the tasks requiring sophisticated path planning and tracking need advanced controls. In order to maintain acceptable performance across a larger range of joint configurations, one might consider utilizing a gain scheduling PID controller, such as presented in [3, 4]. While these controllers can theoretically achieve desirable performance under such circumstances, most implementations of these controllers will require determining acceptable PID gains for multitude of linearized models at different operating conditions. For a 7 DOF manipulator tracking an arbitrary trajectory, the number of such linearizations required will be too large and cumbersome. Additionally, such a method would not account for an unknown end-effector mass. As society looks towards the use of robot manipulators that can interact with humans in social interactions, in rescue operations, and in potential medical applications, the requirement that such manipulators must adhere to an arbitrary desired trajectory during motion becomes an important task. The decentralized adaptive control approach presented here provides one effective control strategy for high performance robot operations for which PID control might not give desirable performance. Such an approach retains much of the simplicity and computational efficiency of the decentralized PID approach, while offering a wide range of applicability with extended joint configuration space and variability of end-effector masses.

Due to the strength of the dynamic interconnection between joints, a model-based approach in which the system is split into a set of decoupled systems is not feasible for robot manipulators. Instead, there are several different methods designed to work around this constraint to achieve a desirable performance. First of all, neural network based methods [5, 6], as well as the disturbance observer method by Yang *et al.* [7], and model-reference method such as by Sundareshan and Koenig [8], attempt to obtain a model of certain system behaviors during the operation of the robot manipulator. Such adaptive-model based methods do not suffer from unmodeled system dynamics, and are well suited for tasks in which the joint dynamics change during the operation of a task. Another popular approach to the decentralized adaptive control of robot manipulators is the model-free approach [9–12], in which the adaptive control law is governed purely from the performance of the manipulator in the tracking task. Model-free approaches, such as that by Seraji [9], can bear strong similarity to the decentralized PID approach. In such approaches, the static gains associated with the PID approach are replaced with adaptive gains, that change during the execution of the task to better track the desired trajectory. Other research efforts for decentralized control of various systems can be found in [13–29].

The goal of this paper is to develop control formulation and conduct experimental verification of the model-free decentralized adaptive method using Baxter, a 7-DOF redundant robot manipulator. This work is novel in that a decentralized adaptive control with experimental verification of a 7-DOF manipulator is not addressed in the literature. The decentralized adaptive control of such a manipulator is an important and challenging task. The increased degrees of freedom of the robot manipulator leads to an increased complexity of dynamic models, which is a challenge for decentralized approaches. Also, the Baxter arm configuration is a more likely choice for the complex tasks to be performed in an industrial setting. Through the analytical formulation and experimental verification of the decentralized adaptive approach, we seek to demonstrate the feasibility and computational effectiveness of said approach, in order to facilitate its adoption into industry practices.

The paper is organized as follows. In Section 2, we present a brief overview of the dynamics of Baxter's right manipulator. Additionally, we also present a decentralized model of Baxter's joint dynamics, as well as the structure of the model-free decentralized adaptive approach. In Section 3.1, we utilize Lyapunov's method to derive the update law for the adaptive gains of the controller, demonstrating asymptomatic stability in the process. In Section 4, we demonstrate and analyze the performance of the decentralized adaptive approach on a simulation of Baxter executing the desired trajectory, paying close attention to tracking performance, controller effort, and selecting adaptive gains. In Section 5, we repeat the same procedure on the Baxter robot in practice, and thoroughly compare the experimental performance to that derived from the simulation. Finally, in Section 6, we

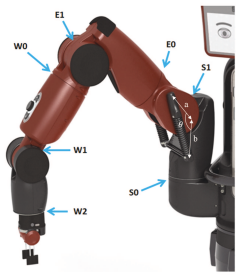

FIGURE 1. The 7-DOF Baxter's arm

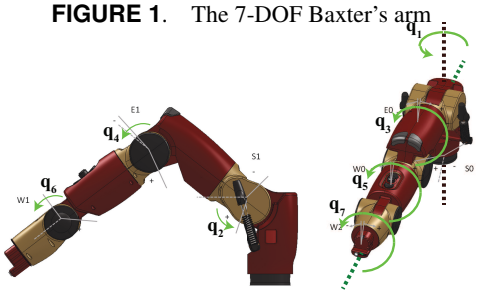

(a) (b)

FIGURE 2. The joints' configuration: (a) sagittal view; (b) top view

present the case that the decentralized adaptive method is computationally efficient, simple to implement, effective at tracking a desired trajectory, and is a desirable alternative to decentralized PID and centralized control for robot manipulators.

2 Mathematical Modeling

The redundant manipulator, which is being studied here, has 7-DOF as shown in Fig. 1. The Baxter manipulator's Denavit-Hartenberg parameters are shown in Table 1 provided by the manufacturer. The Euler-Lagrange formulation leads to a set of 7 coupled nonlinear second-order ordinary differential equations:

$$M(q)\ddot{q}+C(q,\dot{q})\dot{q}+G(q)=\tau+\tau_f(\dot{q}) \tag{1}$$

where, $q,\dot{q},\ddot{q}\in\mathbb{R}^7$ are angles, angular velocities and angular accelerations of joints, respectively, and $\tau\in\mathbb{R}^7$ indicates the vector of joints' driving torques. Also, $M(q)\in\mathbb{R}^{7\times7}$ is a symmetric mass-inertia matrix, $C(q,\dot{q})\in\mathbb{R}^{7\times7}$ is a matrix of Coriolis coefficients, $G(q)\in\mathbb{R}^7$ is a vector of gravitational loading, and $\tau_f(\dot{q})\in\mathbb{R}^7$ represents a vector of frictional torques. For the purpose of simulation, the frictional torque τ_f is modeled utilizing the hyperbolic tangent function in order to approximate the behavior of Coulomb Friction. Our verified coupled nonlinear dynamic model of the robot [30–37] is used as the basis of the decentralized adaptive approach. Also the following assumption is made for the desired joint trajectories.

Assumption 1. *The desired joint trajectories are designed such that $q_r(t)$, $\dot{q}_r(t)$, and $\ddot{q}_r(t)\in\mathbb{R}^7$ exist and are bounded for all $t\geq0$.*

TABLE 1. Baxter's Denavit-Hartenberg Parameters

Link	a_i	d_i	α_i	q_i
1	0.069	0.27035	$-\pi/2$	q_1
2	0	0	$\pi/2$	$q_2+\pi/2$
3	0.069	0.36435	$-\pi/2$	q_3
4	0	0	$\pi/2$	q_4
5	0.010	0.37429	$-\pi/2$	q_5
6	0	0	$\pi/2$	q_6
7	0	0.3945	0	q_7

2.1 Decentralized Model Formulation

In order to derive the decentralized adaptive controller, it is necessary to model the dynamics of a single joint, rather than the system as a whole. Rewriting (1) as series of 7 differential equations yields:

$$m_{ii}(q)\ddot{q}_i + \left[\sum_{i=1,j\neq 1}^{n} m_{ij}(q)\ddot{q}_j\right] + c_i(q,\dot{q})\dot{q} + g_i(q) = T_i(t) + F_i(\dot{q}) \quad (2)$$

where m_{ij} is the element in the mass matrix located at (i,j), $c_i(q,\dot{q})$ is the ith row of the Coriolis matrix, $g_i(q)$ is the ith element of the gravity vector, $T_i(t)$ is the input torque at joint i, and $F_i(\dot{q})$ is the frictional torque at joint i. Note that this equation represents the angular acceleration at joint i as a function of the input torque only at joint i, and the dynamics of each link $q,\dot{q},\ddot{q}$. Thus, (1) can be reduced to a series of 7 dynamically interconnected SISO systems. In order to further express this concept, we rewrite (2) as:

$$m_{ii}(q)\ddot{q}_i + d_i(q,\dot{q},\ddot{q}) = T_i(t) \quad (3)$$

where $d_i(q,\dot{q},\ddot{q}) = \left[\sum_{i=1,j\neq 1}^{n} m_{ij}(q)\ddot{q}_j\right] + c_i(q,\dot{q})\dot{q} + g_i(q) - F_i(\dot{q})$ represents the dynamic interconnection between joints.

3 Decentralized Adaptive Controller

In order to track an arbitrary desired trajectory, we employ the following decentralized adaptive control structure:

$$T_i(t) = f_i(t) + k_{i1}(t)e_i(t) + k_{i2}(t)\dot{e}_i(t) + z_{i1}(t)\dot{q}_{ri}(t) + z_{i2}(t)\ddot{q}_{ri}(t) \quad (4)$$

where $q_{ri}(t)$ is the desired reference trajectory, $e_i(t) = q_{ri}(t) - q_i(t)$ is the tracking error, and $f_i(t), k_{i1}(t), k_{i2}(t), z_{i1}(t), z_{i2}(t)$ are adaptive control signals to be determined through the application of Lyapunov methods. In this formulation, $f_i(t)$ is termed the auxiliary signal, and is the primary driver of the system state $q_i, \dot{q}_i$ towards the desired trajectory. $k_{i1}(t), k_{i2}(t)$ are adaptive PD gains intended to account for current error in the tracking performance, adjusting to the dynamics of the current joint configuration. Similarly, $z_{i1}(t), z_{i2}(t)$ are adaptive feedforward velocity and acceleration gains, intended to ensure that the joint stays on the desired trajectory.

3.1 Derivation of Update Law

In order to derive the equations of the adaptive control signals, we first make the following assumption:

Assumption 2. *The mass element m_{ii}, and the dynamic interconnection between the joints $d_i(q,\dot{q},\ddot{q})$, are slowly time varying with respect to the desired trajectory $q_{ri}(t)$. That is, $\dot{m}_{ii} \approx 0$ and $\dot{d}_i \approx 0$.*

Utilizing this assumption, the decentralized model (3), and the controller law (4), we can express the model plus controller dynamics as:

$$m\ddot{q} + d = f + k_1 e + k_2 \dot{e} + z_1 \dot{q}_r + z_2 \ddot{q}_r \quad (5)$$

Note that the ith subscript, as well as notations indicating functions of time and joint configuration $(t,q,\dot{q},\ddot{q})$, have been removed for the sake of notational simplicity. This equation can be rearranged to obtain:

$$m\ddot{e} + k_2\dot{e} + k_1 e = d - f - z_1\dot{q}_r + (m - z_2)\ddot{q}_r \quad (6)$$

Furthermore, defining the error state vector as $X = [e, \dot{e}]^T$, (6) can be rewritten in state-space form to obtain:

$$\dot{X} = \begin{bmatrix} 0 & 1 \\ \frac{-k_1}{m} & \frac{-k_2}{m} \end{bmatrix} X + \begin{bmatrix} 0 \\ \frac{d-f}{m} \end{bmatrix} + \begin{bmatrix} 0 \\ \frac{-z_1}{m} \end{bmatrix} \dot{q}_r + \begin{bmatrix} 0 \\ \frac{m-z_2}{m} \end{bmatrix} \ddot{q}_r \quad (7)$$

In order to ensure that the robot manipulator follows the desired trajectory, we define the desired performance of the tracking error $e_s(t)$, which we define with the following 2^{nd} order homogeneous differential equation:

$$\ddot{e}_s + 2\xi\omega_n\dot{e}_s + \omega_n^2 e_s = 0 \quad (8)$$

where ω_n is the natural frequency of the desired performance and ξ is the damping ratio. Similarly to (6), we define the reference state vector $X_s = [e_s, \dot{e}_s]^T$, and rewrite (8) in state space form to obtain:

$$\dot{X}_s = \begin{bmatrix} 0 & 1 \\ -\omega_n^2 & -2\xi\omega_n \end{bmatrix} X_s = AX_s \quad (9)$$

Next, we use the following theorem to prove a crucial property of the reference model (9).

Theorem 1. *Consider the linear state-space model $\dot{x} = Ax$. The equilibrium $x = 0$ is globally asymptotically stable if and only if $\exists P = P^T > 0$, $\exists Q = Q^T > 0$ such that the following Lyapunov equation holds:*

$$PA + A^T P = -Q \tag{10}$$

Since we are free to define ξ and ω_n in such a manner as to ensure (9) is globally asymptotically stable, then by Theorem 1 there exists a unique symmetric positive definite matrix P that solves (11) for the linear system (9). We denote the elements in P:

$$P = \begin{bmatrix} P_1 & P_2 \\ P_2 & P_3 \end{bmatrix} \tag{11}$$

Next, we define $E = X_s - X$, and combine (7) and (9) to obtain the tracking error state-space model:

$$\dot{E} = \begin{bmatrix} 0 & 1 \\ -\omega_n^2 & -2\xi\omega_n \end{bmatrix} E + \begin{bmatrix} 0 & 1 \\ \frac{k_1}{m} - \omega_n^2 & \frac{k_2}{m} - 2\xi\omega_n \end{bmatrix} X + \begin{bmatrix} 0 \\ \frac{f-d}{m} \end{bmatrix} + \begin{bmatrix} 0 \\ \frac{z_1}{m} \end{bmatrix} \dot{q}_r + \begin{bmatrix} 0 \\ \frac{z_2 - m}{m} \end{bmatrix} \ddot{q}_r \tag{12}$$

In order to determine the stability properties of (12), it is first necessary to define a Lyapunov function for the system. For this system, we define the following Lyapunov function:

$$V = E^T PE + Q_0(\frac{f-d}{m} - f^*)^2 + Q_1(\frac{k_1}{m} - \omega_n^2 - k_1^*)^2 + Q_2(\frac{k_2}{m} - 2\omega_n\xi - k_2^*)^2 + Q_3(\frac{z_1}{m} - z_1^*)^2 + Q_4(\frac{z_2 - m}{m} - z_2^*)^2 \tag{13}$$

where $Q_0, ..., Q_4$ are positive scalars, and $f^*, k_1^*, k_2^*, z_1^*, z_2^*$ are functions of time to be determined later. Differentiating (13) with respect to time and applying Assumption 2 yields:

$$\begin{aligned} \dot{V} = &-E^T QE + 2\left(\frac{f-d}{m}\right)\left[Q_0(\frac{\dot{f}}{m} - \dot{f}^*) - r\right] - 2Q_0 f^*\left(\frac{\dot{f}}{m} - \dot{f}^*\right) \\ &+ 2\left(\frac{k_1}{m} - \omega_n^2\right)\left[Q_1(\frac{\dot{k_1}}{m} - \dot{k}_1^*) - re\right] - 2Q_1 k_1^*\left(\frac{\dot{k_1}}{m} - \dot{k_1}^*\right) \\ &+ 2\left(\frac{k_2}{m} - 2\xi\omega_n\right)\left[Q_2(\frac{\dot{k_2}}{m} - \dot{k}_2^*) - r\dot{e}\right] - 2Q_2 k_2^*\left(\frac{\dot{k_2}}{m} - \dot{k_2}^*\right) \\ &+ 2\left(\frac{z_1}{m}\right)\left[Q_3(\frac{\dot{z_1}}{m} - \dot{z}_1^*) - r\dot{q}_r\right] - 2Q_3 z_1^*\left(\frac{\dot{z_1}}{m} - \dot{z_1}^*\right) \\ &+ 2\left(\frac{z_2 - m}{m}\right)\left[Q_4(\frac{\dot{z_2}}{m} - \dot{z}_2^*) - r\ddot{q}_r\right] - 2Q_4 z_2^*\left(\frac{\dot{z_2}}{m} - \dot{z_2}^*\right) \end{aligned} \tag{14}$$

where $r = P_2 e + P_3 \dot{e}$ is the weighted error. Before continuing the derivation, we make note of the following theorem:

Theorem 2. *Let $X \in \mathbb{R}^n = 0$ be an equilibrium point of the system $\dot{x} = f(x)$, and let $V : \mathbb{R}^n \to \mathbb{R}$:*

1. *If $V(0) = 0$, $V(X) > 0\ \forall X \neq 0$, $\dot{V} \leq 0\ \forall X \neq 0$, then $X = 0$ is globally stable*
2. *If $V(X) \to \infty$ as $|| X || \to \infty$, then $V(X)$ is radially unbounded*
3. *If $X = 0$ is stable, $V(X)$ is radially unbounded, and $\dot{V} < 0\ \forall X \neq 0$, then $X = 0$ is globally asymptotically stable*

We first note that per our definition of V in (13), V is both positive when $E \neq 0$ and radially unbounded. Thus, we seek to derive adaptation parameters f, k_1, k_2, z_1, z_2, and undetermined parameters $f^*, k_1^*, k_2^*, z_1^*, z_2^*$ such that $\dot{V}$ is negative definite, and thus $E = 0$ is globally asymptotically stable. First, we set the following terms in (14) to 0:

$$\begin{aligned} &Q_0(\frac{\dot{f}}{m} - \dot{f}^*) - r = 0, \quad Q_1(\frac{\dot{k_1}}{m} - \dot{k}_1^*) - re = 0 \\ &Q_2(\frac{\dot{k_2}}{m} - \dot{k}_2^*) - r\dot{e} = 0, \quad Q_3(\frac{\dot{z_1}}{m} - \dot{z}_1^*) - r\dot{q}_r = 0 \\ &Q_4(\frac{\dot{z_2}}{m} - \dot{z}_2^*) - r\ddot{q}_r = 0 \end{aligned} \tag{15}$$

Substituting (15) into (14) yields the following equation:

$$\dot{V} = -E^T QE - 2f^* r - 2k_1^* re - 2k_2^* r\dot{e} - 2z_1^* r\dot{q}_r - 2z_2^* r\ddot{q}_r \tag{16}$$

We then define the following terms:

$$\begin{aligned} f^* &= Q_0^* r \quad & k_1^* &= Q_1^* re \quad & k_2^* &= Q_2^* r\dot{e} \\ z_1^* &= Q_3^* r\dot{q}_r \quad & z_2^* &= Q_4^* r\ddot{q}_r \end{aligned} \tag{17}$$

where $Q_0^*, ..., Q_4^*$ are positive scalars. Substituting (17) into (16) yields:

$$\dot{V} = -E^T QE - 2Q_0^* r^2 - 2Q_1^* r^2 e^2 - 2Q_2^* r^2 \dot{e}^2 - 2Q_3^* r^2 \dot{q}_r^2 - 2Q_4^* r^2 \ddot{q}_r^2 \tag{18}$$

which is negative for all $E \neq 0$, thus Theorem 2 is satisfied and $E = 0$ is globally asymptotically stable. However, we must now determine the values of the parameters f, k_1, k_2, z_1, z_2 to satisfy (15), which are as follows:

$$
\begin{aligned}
\dot{f} &= mQ_0^*\dot{r} + \frac{m}{Q_0}r \\
\dot{k}_1 &= mQ_1^*\frac{d}{dt}(re) + \frac{m}{Q_1}re \\
\dot{k}_2 &= mQ_2^*\frac{d}{dt}(r\dot{e}) + \frac{m}{Q_2}r\dot{e} \\
\dot{z}_1 &= mQ_3^*\frac{d}{dt}(r\dot{q}_r) + \frac{m}{Q_3}r\dot{q}_r \\
\dot{z}_2 &= mQ_4^*\frac{d}{dt}(r\ddot{q}_r) + \frac{m}{Q_4}r\ddot{q}_r
\end{aligned} \tag{19}
$$

We then define the following terms so that (19) is independent of m:

$$
\begin{aligned}
Q_0^* &= \frac{\rho}{m} \quad Q_0 = \frac{m}{\delta} \\
Q_1^* &= \frac{\beta_1}{m} \quad Q_1 = \frac{m}{\alpha_1} \\
Q_2^* &= \frac{\beta_2}{m} \quad Q_2 = \frac{m}{\alpha_2} \\
Q_3^* &= \frac{\lambda_1}{m} \quad Q_1 = \frac{m}{\gamma_1} \\
Q_4^* &= \frac{\lambda_2}{m} \quad Q_2 = \frac{m}{\gamma_2}
\end{aligned} \tag{20}
$$

Substituting (20) into (19) and integrating with respect to time yields the following equations for the decentralized adaptive parameters:

$$
\begin{aligned}
f(t) &= f(0) + \delta\int_0^t r(t)dt + \rho r(t) \\
k_1(t) &= k_1(0) + \alpha_1\int_0^t r(t)e(t)dt + \beta_1 r(t)e(t) \\
k_2(t) &= k_2(0) + \alpha_2\int_0^t r(t)\dot{e}(t)dt + \beta_2 r(t)\dot{e}(t) \\
z_1(t) &= z_1(0) + \gamma_1\int_0^t r(t)\dot{q}_r(t)dt + \lambda_1 r(t)\dot{q}_r(t) \\
z_2(t) &= z_2(0) + \gamma_2\int_0^t r(t)\ddot{q}_r(t)dt + \lambda_2 r(t)\ddot{q}_r(t)
\end{aligned} \tag{21}
$$

Now that we have successfully derived the decentralized adaptive gains, we make the following notes of its structure. First of all, the auxiliary signal can be interpreted as a decentralized PID signal, acting to guide the system towards the desired trajectory in a generalized approach. Second of all, each adaptive gain is updated based on the performance of the signal it multiplies in (4), as well as the weighted error. This update law is purely performance based, and does not rely on a model of the system. Finally, the update of each parameter is a simple computation, where a trapezoidal approximation can be used to estimate the value of the integral at each time step.

4 Simulation Results

In order to assess the performance of this decentralized adaptive controller, we first apply the control law described in Section 3 to the Baxter's dynamic model (1). We apply our control methodology to a tracking problem where the desired tracking trajectories for the joints were created for a specific end-effector maneuver in [36]. While the maneuver was a pick-and-place task in [36] in which the desired joint trajectories were generated online, for our problem our interest is in using these previously generated trajectories as a reference for tracking. In this simulation, we introduce a sampling rate of 100 Hz in order to effectively model the effect of discrete sampling on the continuous-time controller. Furthermore, the controller parameters we used during this simulation, can be observed in Table 2.

TABLE 2. Controller Parameters for Simulation and Experiment

Joint	1	2	3	4	5	6	7
p_{i2}	1	1	1	1	1	1	1
p_{i3}	0.3	0.3	0.3	0.3	0.3	0.3	0.3
δ_i	30	60	40	30	7	40	2
ρ_i	30	60	40	30	7	6	2
α_{i1}	6000	6000	6000	6000	10200	102000	1200
β_{i1}	600	600	600	600	1020	10200	120
α_{i2}	6	6	6	6	6	6	6
β_{i2}	0.6	0.6	0.6	0.6	0.6	0.6	0.6
γ_{i1}	60	60	60	60	60	60	60
λ_{i1}	6	6	6	6	6	6	6
γ_{i2}	60	60	60	60	60	60	60
λ_{i2}	6	6	6	6	6	6	6

The simulated joint trajectories, along with the desired joint trajectories can be observed in Figure 3. From these graphs, it can be seen that the decentralized adaptive controller achieves close tracking of the desired trajectories. Although the effects of the simulated frictional torque and gravity negligibly impact the tracking performance during the beginning of motion, as can be seen in the performance of joints 3, 5, and 6, these effects are quickly accounted for by the adaptive controller. Furthermore, despite large changes in the joint configuration throughout the course of the operation, the performance based control scheme remains effective at consistently driving each joint towards the

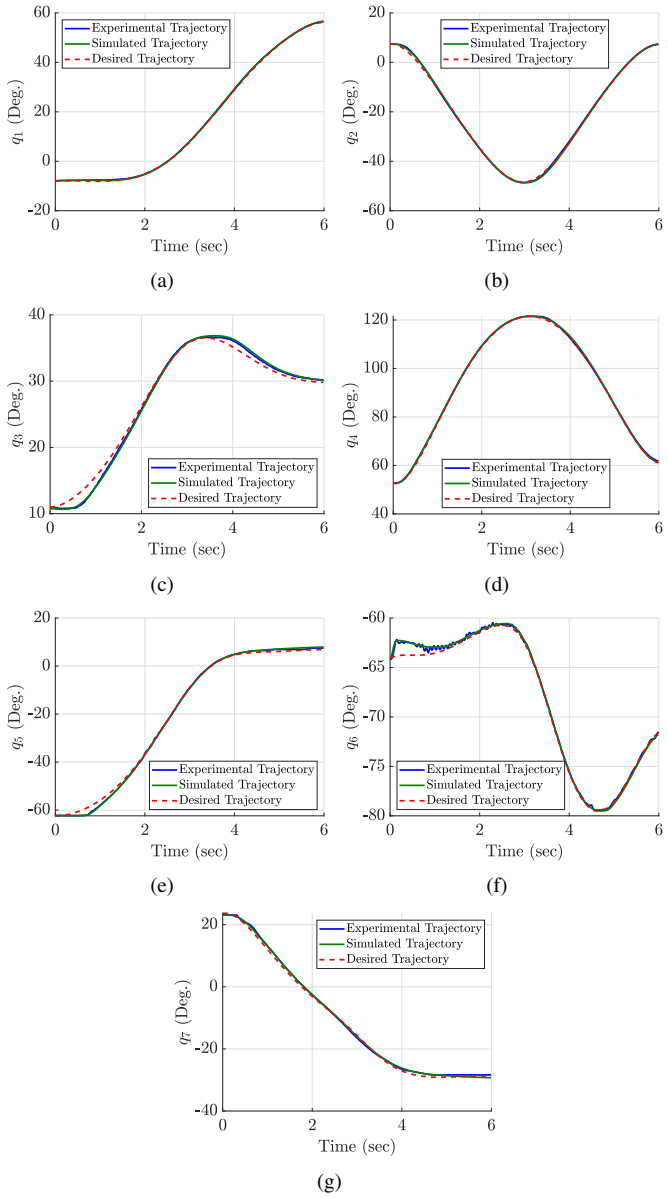

FIGURE 3. The experimental (blue line), simulated (green line), and desired (red dashed line) joint trajectories of Baxter

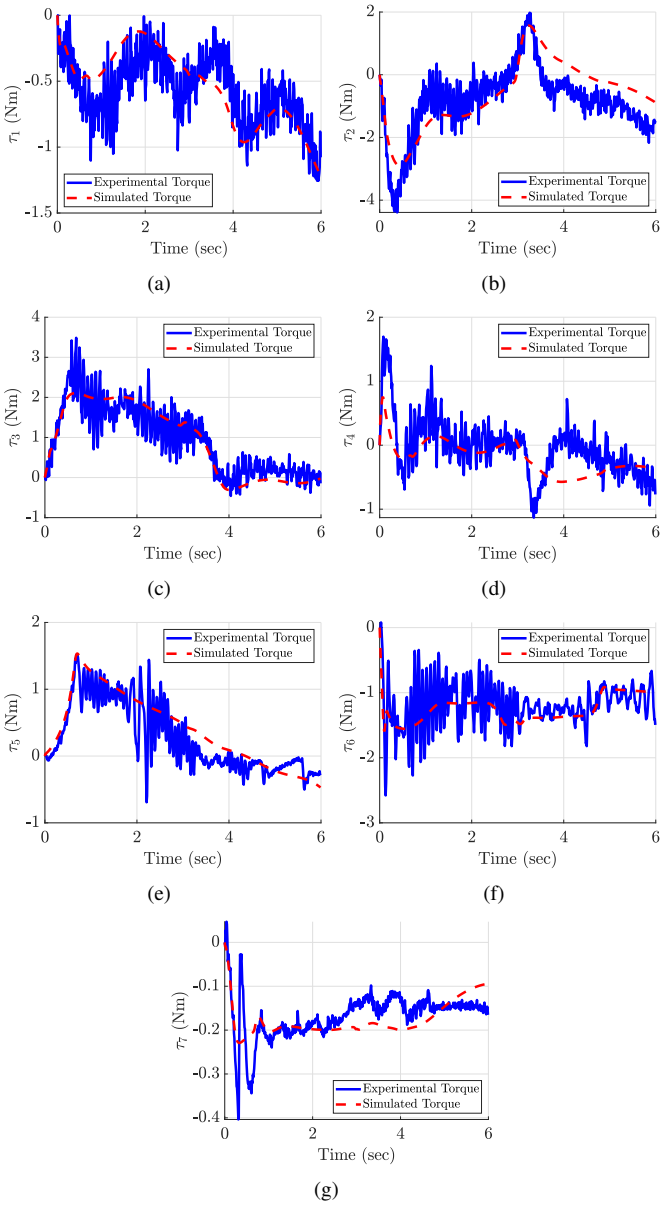

FIGURE 4. The experimental (blue line) and simulated (red dashed line) joint torques of Baxter

desired trajectory. These behaviors can also be observed in Figure 6, as the tracking error remains less than 1.5 degrees for all joints after 1.5 seconds of operation.

The torques generated by the decentralized adaptive controller can be observed in Figure 4. It is important to note that these torques are significantly lower than the maximum torque output of Baxter's joints, which are 50 Nm for joints 1-4, and 15 Nm for joints 5-7, meaning that saturation of torque is not an issue for this decentralized adaptive scheme. Furthermore, this demonstrates energy efficiency of this control scheme, as the torques generated are consistently small in magnitude. Additionally, it can be observed that the torques generated are smooth throughout the operation, which is potentially beneficial to the motors that are used to generate these torques in practice.

Finally, we observe the tuning of adaptive gains k_1 through the simulation, as seen in Figure 5. Each of these gains appear to adjust in 2 stages ($0s < t < 3s$ and $3s < t < 6s$). These phases correspond to the picking up and placing down motion of the end manipulator, signifying that a different set of gains is necessary for each task. Thus, the tuning of these parameters coincide with our expectations of their performance. It is also important to note

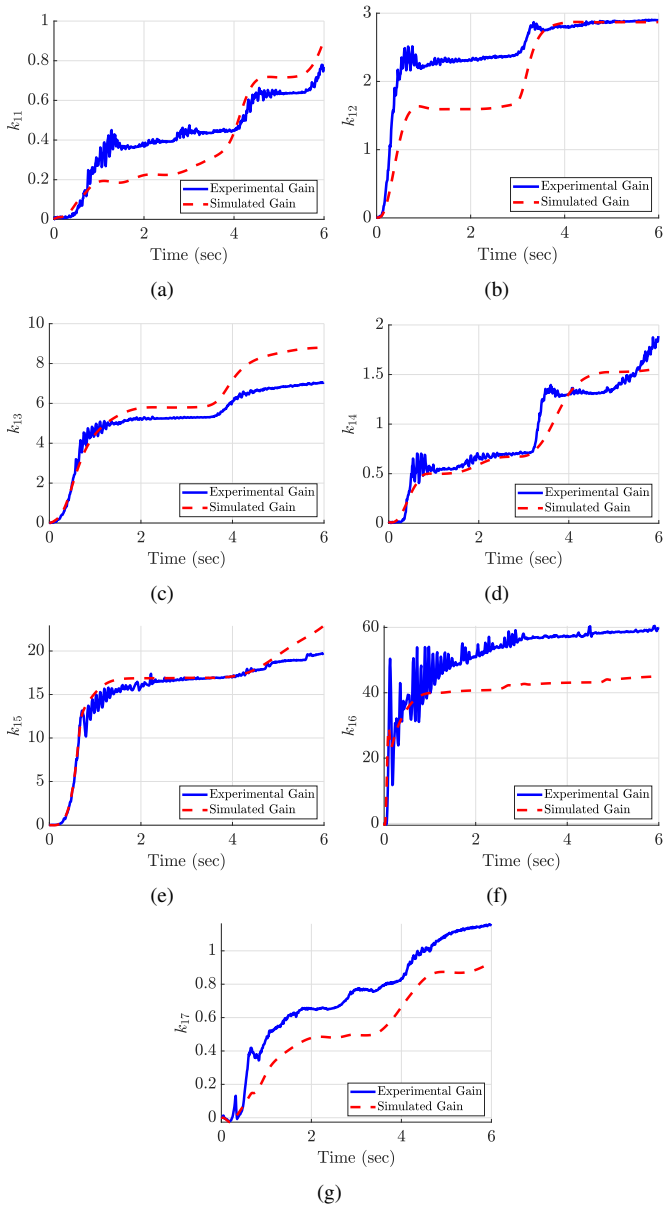

FIGURE 5. The tuning of adaptive gain k_1 during experimentation (blue line) and simulation (red dashed line) of Baxter

that these gains are of a significant magnitude when compared to the auxiliary parameters δ_i and ρ_i, meaning that tunings were necessary in order to achieve the desired tracking performance. Furthermore, the joints 3, 5, and 6 with significantly tuned gains experienced the largest frictional torques and gravitational load. These results demonstrate the ability of the decentralized adaptive controller to adjust to different operating conditions. This beneficial quality of this scheme is of key importance when the robot manipulator is expected to reliably perform in a changing environment. From these results, it is evident that the decentralized adaptive controller is effective in simulation.

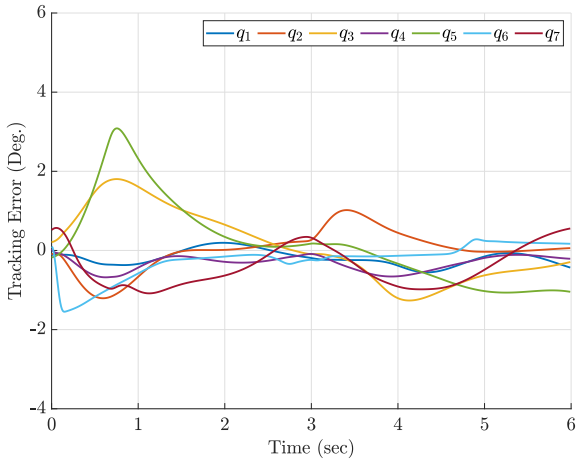

FIGURE 6. Simulated tracking error

5 Experimental Results

Due to promising results during simulation, we now implement the control law described in Section 3 to Baxter in an experimental study. We utilize the same desired trajectories as in Section 4 with the same 100 Hz sampling rate. Note that several differences remain between the simulated and experimental study, which include measurement noise in the joint positions and velocities, differences between the idealistic Coulomb Friction model and the actual friction dynamics, small potential inaccuracies in model parameters, and the actuator dynamics of each joint. These factors can lead to results slightly different than those experienced in simulation. For the experimental pick-and-place task, the controller parameters we used are the same as that of the simulation, and can be observed in Table 2.

From Figure 7(a), it can be observed that the decentralized adaptive controller is successful at executing the pick-and-place task in practice. The experimental joint trajectories, along with the desired joint trajectories can be observed in Figure 3. From these graphs, it can be seen that the decentralized adaptive controller exhibits close tracking of the desired trajectory, that is almost identical to that experienced during simulation. Similar to the Experiment, it can be observed from the graphs that errors experienced in the beginning of the operation are quickly accounted for, and the controller returns to near perfect tracking. This behavior can also be observed in Figure 8, as the tracking error remains less than 1.5 degrees after 1.5 seconds of operation.

The torques generated by the decentralized adaptive controller can be observed in Figure 4. While the presence of noise in measurements has caused similar variations in the joint torques, the torques still exhibit moderate continuity, as well as a magnitude much less than the saturation torque of each joint.

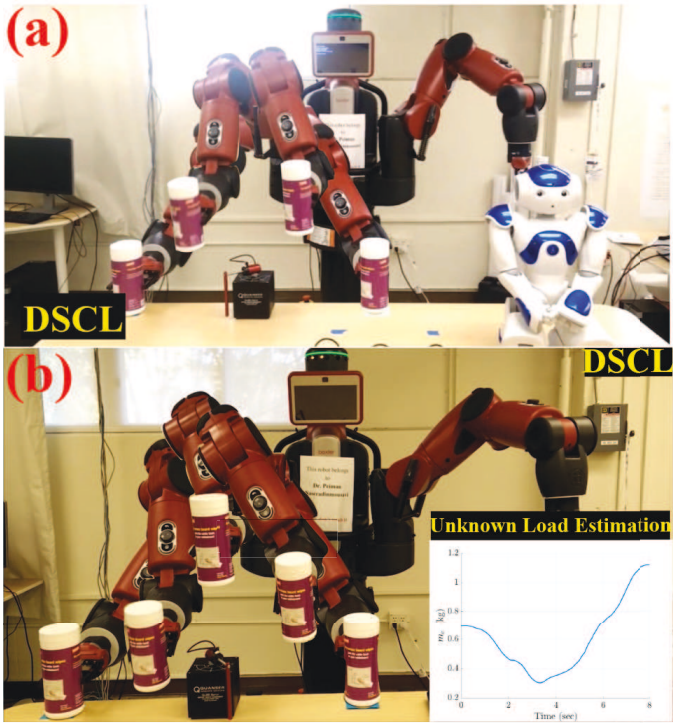

FIGURE 7. Baxter tracking a desired trajectory under (a) the decentralized adaptive and (b) model-based centralized adaptive control schemes at Dynamic Systems and Control Laboratory (DSCL); see peimannm.sdsu.edu

It can be seen from these graphs that the overall shape and magnitude of the experimental torque of each joint matches closely to that of the corresponding simulated torques. Thus, the differences in system dynamics between the simulation and experiment do not significantly affect the performance of the decentralized control algorithm.

Finally, we observe the tuning of the adaptive gains k_{1i} through the experiment, as seen in Figure 5. The behavior of these graphs is similar to that of the simulation in regards to both the stages of tuning, as well as the magnitude of the gains. Slight differences can be observed between the evolution of the gains in the simulation and experiment, which can reasonably be attributed to the small differences in dynamics between the simulated and actual system, such as the difference between the idealistic Coulomb Friction model from the friction experienced in the real system. While these differences lead to the selection of different gains from simulation, the overall performance of the decentralized adaptive controller is not significantly affected by this difference in dynamics, as can be seen in Figures 3 and 4. Thus, these adaptive gains are effective at maintaining desirable performance outside of the conditions in which the decentralized adaptive controller was designed. From these results, it is evident that the decentralized adaptive scheme performs well in experiments as well as in simulation.

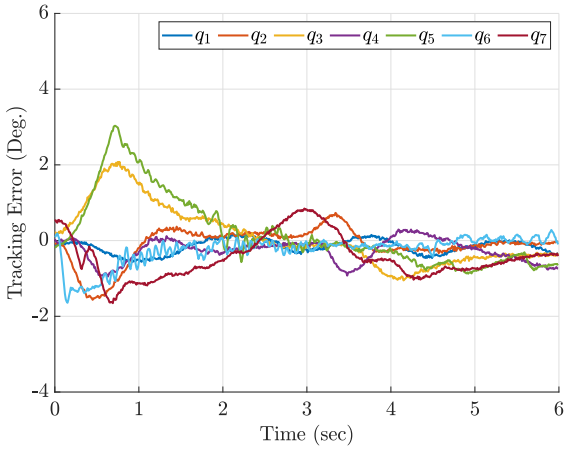

FIGURE 8. Experimental tracking error

Another crucial point to consider is the computational efficiency of the decentralized adaptive scheme compared to centralized ones. We previously carried out experimental work for a simple centralized model-based adaptive scheme to carry an unknown mass avoiding an obstacle, shown in Fig. 7(b). The mass of the end-effector was the only unknown parameter to be estimated and we again employed the Damped Least Squares method to calculate desirable joint-space trajectories. The immediate challenge was the computation time of the control scheme in each loop, even when dealing with only one uncertainty, which was incompatible with the minimum time step ($\Delta t_b = 0.001s$ or $f_b = 1kHz$) of Baxter. The computation time of the centralized model-based adaptive scheme was in the range of $\mathbf{0.005s} \leq t_c \leq \mathbf{0.007s}$ leading to the time delay in each control loop. Therefore, we had to address a critical trade-off between the accuracy required and computational cost. To resolve this problem, we increased the Baxter's time step to $\Delta t_b = 0.01s$ or $f_b = 0.1kHz$, along with the sleep command of Python, in order to avoid such a time delay by sacrificing the accuracy needed. Shown in Fig. 7(b) is the experimental implementation of the centralized adaptive control of Baxter carried out at the DSC laboratory. We noticed that the estimation of even one uncertainty, without any external disturbance, caused at least three small operational interruptions. Please check the DSCL YouTube Channel, at https://youtu.be/4XWldAXpJ2I, for the AVI file. Note that the decentralized adaptive scheme examined here reveals a significantly lower computation time of $\Delta t_b = \mathbf{1.02\ ms}$ compared to the centralized one. Therefore, we did not observe the operational interruptions discussed for the centralized method whereas the decentralized scheme is at least five times faster than the centralized one. This would be highly beneficial for when we intend to control large-scale (high-DOF) systems.

6 Conclusion

In this paper, we investigated the performance of a model-free decentralized adaptive controller on a 7-DOF redundant manipulator. We first formulated the theory behind the controller, demonstrating the global asymptotic stability of each local controller, as well as revealing the computationally efficient method of adapting each control parameter. Then, through the results of both our simulation and experiment of the decentralized adaptive controller implemented on Baxter, we demonstrated the following beneficial properties of the control scheme:

1. The algorithm is highly computationally efficient and at least five times faster than the centralized adaptive method examined here.
2. Close tracking of the desired trajectory is achieved throughout operation.
3. Large changes in the joint configuration throughout the procedure do not significantly affect the operation.
4. The generated torques are energy efficient, and do not pose the risk of torque saturation.
5. The control scheme can adapt to, and is effective outside of the conditions in which it was designed for.

Thus, we verified the effectiveness of the model-free decentralized adaptive control scheme, and noted its promising potential for a wide variety of applications.

Acknowledgment

This article is based upon work supported by the National Science Foundation under Award #1823951. The views and opinions of authors expressed herein do not necessarily state or reflect those of the United States Government or any agency thereof.

References

[1] Alvarez-Ramirez, J., Santibanez, V., and Campa, R., 2008. "Stability of robot manipulators under saturated pid compensation". *IEEE Transactions on Control Systems Technology,* ***16***(6), Nov, pp. 1333–1341.

[2] Youngjin Choi, Wan Kyun Chung, and Il Hong Suh, 2001. "Performance and h/sub /spl infin// optimality of pid trajectory tracking controller for lagrangian systems". *IEEE Transactions on Robotics and Automation,* ***17***(6), Dec, pp. 857–869.

[3] Jarrah, M. A., and Al-Jarrah, O. M., 1999. "Position control of a robot manipulator using continuous gain scheduling". In Proceedings 1999 IEEE International Conference on Robotics and Automation (Cat. No.99CH36288C), Vol. 1, pp. 170–175 vol.1.

[4] Ya Lei Sun, and Meng Joo Er, 2004. "Hybrid fuzzy control of robotics systems". *IEEE Transactions on Fuzzy Systems,* ***12***(6), pp. 755–765.

[5] Karakasoglu, A., Sudharsanan, S. I., and Sundareshan, M. K., 1993. "Identification and decentralized adaptive control using dynamical neural networks with application to robotic manipulators". *IEEE Transactions on Neural Networks,* ***4***(6), Nov, pp. 919–930.

[6] Tan, K. K., Huang, S., and Lee, T. H., 2009. "Decentralized adaptive controller design of large-scale uncertain robotic systems". *Automatica,* ***45***(1), pp. 161–166.

[7] Yang, Z., Fukushima, Y., and Qin, P., 2012. "Decentralized adaptive robust control of robot manipulators using disturbance observers". *IEEE Transactions on Control Systems Technology,* ***20***(5), Sep., pp. 1357–1365.

[8] Sundareshan, M. K., and Koenig, M. A., 1985. "Decentralized model reference adaptive control of robotic manipulators". In 1985 American Control Conference, IEEE, pp. 44–49.

[9] Seraji, H., 1989. "Decentralized adaptive control of manipulators: theory, simulation, and experimentation". *IEEE Transactions on Robotics and Automation,* ***5***(2), April, pp. 183–201.

[10] Colbaugh, R., Seraji, H., and Glass, K., 1994. "Decentralized adaptive control of manipulators". *Journal of Robotic Systems,* ***11***(5), pp. 425–440.

[11] Tarokh, M., 1996. "Decentralized adaptive tracking control of robot manipulators". *Journal of robotic systems,* ***13***(12), pp. 803–816.

[12] Liu, M., 1999. "Decentralized control of robot manipulators: nonlinear and adaptive approaches". *IEEE Transactions on Automatic control,* ***44***(2), pp. 357–363.

[13] Chen, Y. H., 1991. "Decentralized adaptive robust control design: The uncertainty is time varying". *Journal of Dynamic Systems, Measurement, and Control,* ***113***(3), sep, pp. 515–518.

[14] Hua, C., Guan, X., and Shi, P., 2005. "Robust decentralized adaptive control for interconnected systems with time delays". *Journal of Dynamic Systems, Measurement, and Control,* ***127***(4), mar, pp. 656–662.

[15] Lyou, J., and Bien, Z., 1985. "Decentralized adaptive stabilization of a class of large-scale interconnected discrete systems". *Journal of Dynamic Systems, Measurement, and Control,* ***107***(1), mar, pp. 106–109.

[16] Li, Y., Lu, Z., Zhou, F., Dong, B., Liu, K., and Li, Y., 2019. "Decentralized trajectory tracking control for modular and reconfigurable robots with torque sensor: Adaptive terminal sliding control-based approach". *Journal of Dynamic Systems, Measurement, and Control,* ***141***(6), feb.

[17] Hernández-Alemán, R., Salas-Peña, O., and León-Morales, J. D., 2017. "Decentralized formation control based on adaptive super twisting". *Journal of Dynamic Systems, Measurement, and Control,* ***139***(4), feb.

[18] Watanabe, K., 1989. "A decentralized multiple model adaptive filtering for discrete-time stochastic systems". *Journal*

of Dynamic Systems, Measurement, and Control, ***111***(3), sep, pp. 371–377.

[19] Yan, J.-J., 2003. "Memoryless adaptive decentralized sliding mode control for uncertain large-scale systems with time-varying delays". *Journal of Dynamic Systems, Measurement, and Control,* ***125***(2), jun, pp. 172–176.

[20] Hashemipour, S. H., Vasegh, N., and Sedigh, A. K., 2017. "Decentralized MRAC for large-scale interconnected systems with state and input delays by integrators inclusion". *Journal of Dynamic Systems, Measurement, and Control,* ***139***(9), jun.

[21] Elmahdi, A., Taha, A. F., Sun, D., and Panchal, J. H., 2015. "Decentralized control framework and stability analysis for networked control systems". *Journal of Dynamic Systems, Measurement, and Control,* ***137***(5), may.

[22] Ghasemi, A. H., Hoagg, J. B., and Seigler, T. M., 2016. "Decentralized vibration and shape control of structures with colocated sensors and actuators". *Journal of Dynamic Systems, Measurement, and Control,* ***138***(3), jan.

[23] Yeatman, M., Lv, G., and Gregg, R. D., 2019. "Decentralized passivity-based control with a generalized energy storage function for robust biped locomotion". *Journal of Dynamic Systems, Measurement, and Control,* ***141***(10), jun.

[24] Wang, C., and Li, D., 2011. "Decentralized PID controllers based on probabilistic robustness". *Journal of Dynamic Systems, Measurement, and Control,* ***133***(6), nov.

[25] Kalat, S. T., Faal, S. G., and Onal, C. D., 2018. "A decentralized, communication-free force distribution method with application to collective object manipulation". *Journal of Dynamic Systems, Measurement, and Control,* ***140***(9), apr.

[26] Kan, Z., Klotz, J. R., Shea, J. M., Doucette, E. A., and Dixon, W. E., 2016. "Decentralized rendezvous of nonholonomic robots with sensing and connectivity constraints". *Journal of Dynamic Systems, Measurement, and Control,* ***139***(2), nov.

[27] Pagilla, P. R., and Zhu, Y., 2004. "A decentralized output feedback controller for a class of large-scale interconnected nonlinear systems". *Journal of Dynamic Systems, Measurement, and Control,* ***127***(1), apr, pp. 167–172.

[28] Pavone, M., and Frazzoli, E., 2006. "Decentralized policies for geometric pattern formation and path coverage". *Journal of Dynamic Systems, Measurement, and Control,* ***129***(5), oct, pp. 633–643.

[29] Brahmi, B., Brahmi, A., Saad, M., Gauthier, G., and Rahman, M. H., 2019. "Robust adaptive tracking control of uncertain rehabilitation exoskeleton robot". *Journal of Dynamic Systems, Measurement, and Control,* ***141***(12), sep.

[30] Bagheri, M., and Naseradinmousavi, P., 2017. "Novel analytical and experimental trajectory optimization of a 7-dof baxter robot: global design sensitivity and step size analyses". *The International Journal of Advanced Manufacturing Technology,* ***93***(9-12), December, pp. 4153–4167.

[31] Bagheri, M., Naseradinmousavi, P., and Morsi, R., 2017. "Experimental and novel analytical trajectory optimization of a 7-dof baxter robot: Global design sensitivity and step size analyses". In ASME 2017 Dynamic Systems and Control Conference, Vol. 1, p. V001T30A001.

[32] Bagheri, M., Krstić, M., and Naseradinmousavi, P., 2018. "Joint-space trajectory optimization of a 7-dof baxter using multivariable extremum seeking". In 2018 Annual American Control Conference (ACC), pp. 2176–2181.

[33] Bagheri, M., Krstić, M., and Naseradinmousavi, P., 2018. "Multivariable extremum seeking for joint-space trajectory optimization of a high-degrees-of-freedom robot". *Journal of Dynamic Systems, Measurement, and Control,* ***140***(11), p. 111017.

[34] Bagheri, M., Krstić, M., and Naseradinmousavi, P., 2018. "Analytical and experimental predictor-based time delay control of baxter robot". In ASME 2018 Dynamic Systems and Control Conference, Vol. 1, p. V001T04A011.

[35] Bagheri, M., Naseradinmousavi, P., and Krstić, M., 2019. "Feedback linearization based predictor for time delay control of a high-dof robot manipulator". *Automatica,* ***108***, p. 108485.

[36] Bertino, A., Bagheri, M., Krstić, M., and Naseradinmousavi, P., 2019. "Experimental autonomous deep learning-based 3d path planning for a 7-dof robot manipulator". In ASME 2019 Dynamic Systems and Control Conference, Vol. 2, p. V002T14A002.

[37] Bagheri, M., Naseradinmousavi, P., and Krstić, M., 2019. "Time delay control of a high-DOF robot manipulator through feedback linearization based predictor". In ASME 2019 Dynamic Systems and Control Conference, Vol. 3, American Society of Mechanical Engineers, p. V003T16A001.